Dosimetry and mechanical accuracy of the first rotating gamma system installed in North America

Hideo D. Kubo[a] and Fujio Araki[b]
Department of Radiation Oncology, UC Davis Cancer Center, Sacramento, California 95817

(Received 30 April 2002; accepted for publication 21 August 2002; published 22 October 2002)

The purpose of this paper is to present the dosimetry and mechanical accuracy of the first rotating gamma system (RGS) installed in North America for stereotactic radiosurgery. The data were obtained during the installation, acceptance test procedure, and commissioning of the unit. The RGS unit installed at UC Davis Cancer Center (RGS_u) has modifications on the source and collimator bodies from the earlier version of the Chinese RGS (RGS_c). The differences between these two RGSs are presented. The absolute dose at the focal point was measured in a 16-cm-diam acrylic phantom using a small volume chamber, which was calibrated at the University of Wisconsin Accredited Dosimetry Calibration Laboratory (UW-ADCL). The dose in acrylic was then converted to a dose in water. A collimator output factor from each of the four different collimator sizes ranging from 4, 8, 14, and 18 mm was measured with (1) a smaller volume chamber and (2) approximately 3.0 mm$\times$3.0 mm$\times$1.0 mm TLD chips in the same acrylic phantom. The Gafchromic films were used for the dose profile, collimator output factor, and mechanical/radiation field isocentricity measurements. The TLD chips were processed in-house whereas Gafchromic films were processed both at the UW-ADCL and in-house. The timer error, timer accuracy, and timer linearity were also determined. The dose profiles were found to be similar between RGS_c and RGS_u. The 4 mm collimator output factor of the RGS_u was approximately 0.6, similar to that from RGS_c, in comparison to 0.8 in the report for a Leksell Model U Gamma-Knife. The mechanical/radiation field isocentricity for RGS_c and RGS_u is found to be similar and is within 0.3 mm in both *X* and *Y* directions. In the *Z* direction, the beam center of the RGS_u is shifted toward the sources by 0.75 mm from the mechanical isocenter whereas no data are available for RGS_c. Little dosimetric difference is found between RGS_u and RGS_c. It is reported that RGS_c has the same dosimetric and mechanical characteristics as the Model U Gamma-Knife. Therefore, RGS_u should be capable of achieving stereotactic radiosurgery with the same degree of dosimetric and mechanical accuracy as with the Gamma-Knife. © *2002 American Association of Physicists in Medicine*.
[DOI: 10.1118/1.1514039]

Key words: rotating gamma system, Gamma-Knife, stereotactic, radiosurgery

I. INTRODUCTION

Goetsch *et al.*[1] collected radiation dosimetry data from the Chinese version of the rotating gamma system (RGS_c) at Auhai Radiosurgery Center in Beijing, People's Republic of China. Subsequently they collected dosimetry data from two Leksell model U Gamma-Knives. They published dose comparison data between these two types of gamma units in 1999.[1] The paper included the results obtained with radiochromic films and the ion chamber calibrated by the University of Wisconsin Accredited Dosimetry Calibration Laboratory (UW-ADCL). The chamber they used was a Capintec model PR-05P "mini" chamber (Ramsey, NJ) with a nominal sensitive volume of 0.07 cc. The film was ISP Model HD-810 (Nuclear Associates, Carle Place, NY), single emulsion radiochromic film.[2,3]

A group of physicians and a physicist from the University of California Davis Medical Center visited the same Auhai Radiosurgery Center in Beijing in 1999. The lead author of this paper conducted similar, limited dosimetric and mechanical measurements as Goetsch *et al.*[1] The film was ISP Type MD-55 (Nuclear Associates, Carle Place, NY), triple emulsion radiochromic film. The chamber measurement was done with the 18 mm collimator using the Auhai Radiosurgery Center's PTW-UNIDOS with 0.125 cc sensitive volume. When the new RGS unit was installed at UC Davis Cancer Center (RGS_u), the absolute dose measurement was made with the Capintec PR-05P "mini" chamber for the 14 and 18 mm collimators and with TLD using the MD Anderson stereotactic head phantom for the 18 mm collimator. Relative dosimetric and mechanical comparison between the two RGS units were made as described in Sec. II.

RGS_c has been marketed by OUR Scientific (Pleasanton, CA). The planning software was developed by Northwest Medical Physics (Seattle, WA) and is substantially different from the Chinese version. During the installation of the RGS hardware at UCD Cancer Center, it became apparent that the following advantages were realized by sacrificing some delay in the acceptance test procedure and commissioning. The unit could be mechanically modified on site (1) to allow the treatment target to be 3 cm inferior to RGS_c and (2) for the future application of IMRT. These modifications involved reboring of the primary and secondary source collimator bod-

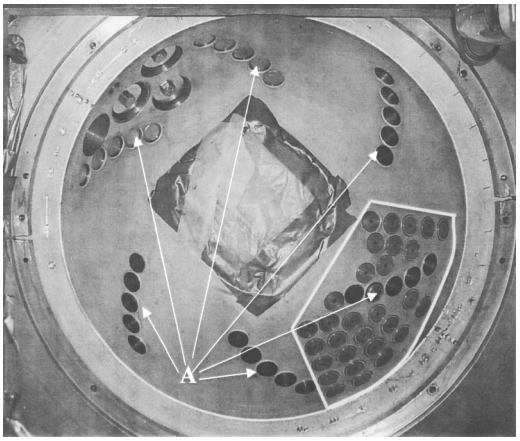

FIG. 1. Primary collimator body. Six arrows indicate the locations of the original source containing cylinder bores, two of which are already plugged. All of them are eventually plugged. The white enclosure in the lower right-hand corner is the new source cluster.

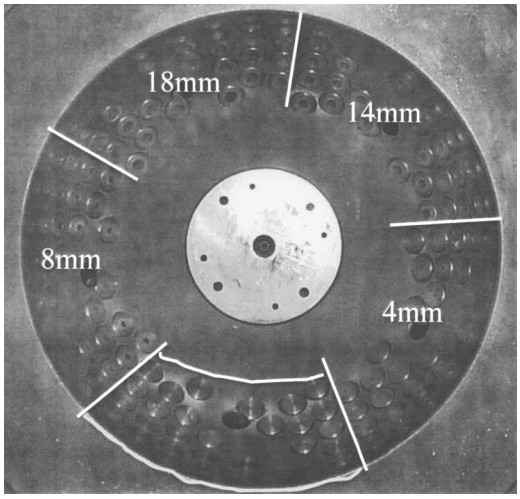

FIG. 2. Secondary collimator body. Five sets of collimators are arranged from the bottom. They are shown clockwise from the bottom, the blocked, 8, 18, 14, and 4 mm collimators.

ies. The shift of the focal spot by 3 cm inferior was designed to treat further inferior tumors than the original RGS could achieve. This shift may inadvertently increase the dose inferior to the target in comparison to the original RGS. Since this potential dose increase depends on many factors including the target size, collimator size, and the locations of the targets, no study is made to ascertain such an increase. A source rotation speed is made variable so that each treatment gives a multiple of complete revolutions as discussed later. When the selected collimator is docked with the source body, the timer on the control unit will start. The docked system will continue to rotate together until the treatment is completed. During the treatment a portion of the rotation can be docked or undocked by the RGS control software, or can have a different collimator size by adjusting the secondary collimator rotation speed, thus allowing varying radiation dose distributions. This potential IMRT dose delivery capability is another reason for the modifications. However, the software for this feature has not yet been developed and will not be discussed any further in this paper.

All other features are the same as RGS_c. Therefore, only details of the modifications are described in this paper and the general features of the RGS are described as needed. Since Goetsch *et al.*[1] compared some dosimetric and mechanical differences between RGS_c and the Gamma-Knife, this work only compares the differences between the two different types of RGS.

Specifically, the modifications involved plugging the original source cylinder and secondary collimator, and reboring of the new source containing cylinders on the primary collimator body and reboring of the matching collimator on the secondary collimator body. Figure 1 is a photo of the primary collimator. The original location of the six groups of five source cylinders arranged in a spiral curvature, each separated from one another by 60°, is indicated by arrows. Because of this source configuration, RGS_c provides the dosimetric symmetry about the source rotation axis. Duct tape shown in the center of the photo was used to keep dust away during the boring.

Figure 1 also shows the modified primary collimator body with the source bores clustered in the lower right-hand side of the figure as indicated in the white enclosure. Thirty dummy source cylinders were inserted into the new source bores. Unlike the Gamma-Knife, which utilizes 201 Co-60 sources of approximately 1.11×10^{12} Bq, a RGS system uses 30 sources of approximately 7.4×10^{12} Bq each. At the time of the source certification measurement at International Isotopes Idaho (Idaho Falls, ID) on 14 December 1999, the total activity was reported to be 2.22×10^{14} Bq with $\pm5\%$ uncertainty. Toward the upper left-hand corner, one can see four larger bores with three of them being plugged. These tungsten plugs are added to counter-balance the extra weight created by clustering tungsten source cylinders in one corner. The source configuration is no longer axially symmetric. The new source cylinder bores are drilled in such a way that the angle between the central axis of the bore and the vertical axis in the sagittal plane changed from the Chinese version of 14°–43° (Ref. 1) to 15°–52°. The Gamma-Knife has an angle span of 15°–45°.

Figure 2 shows the secondary collimator body. One can identify five sets of clusters. Each collimator cluster is made up of collimator sizes ranging from 4, 8, 14, to 18 mm diameters, including a completely blocked one seen in the white enclosure. This blocked collimator functions as the secondary shutter. Normally the source cluster docked with the blocked collimator is located at the bottom of the shielded housing called a ''home position'' when the unit is not in use. This position produces the lowest leakage around the unit. When the treatment button is pushed, the source cluster docked with the blocked collimator starts rotating together until they reach and maintain a precalculated speed of between 1.0 and 2.0 rpm. At the same time, the shielding door opens and the couch moves in. When the couch is docked for treatment, the secondary collimator rotation starts

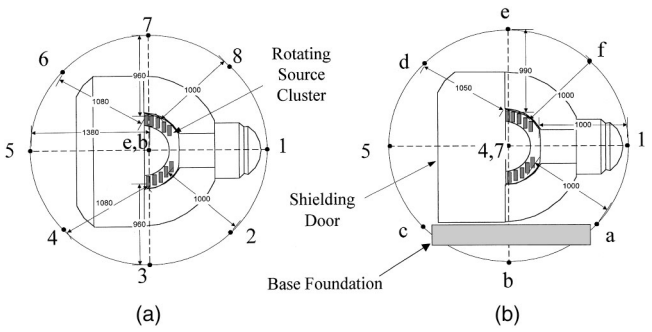

FIG. 3. Leakage radiation measurement locations around the source housing at approximately 1 m from the focal spot: Top view (a) and side view (b).

either slowing down or speeding up until the source cluster docks with the selected collimator. For example, prior to irradiation, either the 8 or 18 mm collimator cluster will speed up and will dock with the source cluster, or the 4 or 14 mm collimator cluster will slow down and will dock with the source cluster. This means that when the 14 or 18 mm collimator is selected, the 4 or 8 mm collimator cluster is matched in transient with the source cluster, thus briefly irradiating the patient before reaching the selected collimator of 14 or 18 mm. This transient dose was estimated to be much less than 1.0 cGy, too small to be included in the treatment plan calculations.

Another modification that is incorporated into RGS_u is the variable source rotation speed. When the treatment time is entered into the controller, the controller will determine the source rotation speed so as to yield a multiple of complete revolutions. In this way the axial symmetry of the dose distribution is maintained. In order to complete at least one full revolution, the minimum treatment time is approximately 30 s.

II. METHODS AND MATERIALS

A. Dosimetry

The absolute dosimetry was performed with the two in-house dosimetry systems, i.e., an ion chamber calibrated at the UW-ADCL, and thermoluminescent dosimeter (TLD). The chamber was a Capintec Model PR-05P "mini" chamber. The chamber was inserted into a slot drilled in a 16-cm-diam and 1-cm-thick acrylic plate, which itself was inserted into a 16-cm-diam spherical acrylic phantom. The chamber's long axis coincided with the source rotation axis to maintain the dosimetric symmetry. Since the RGS_u Co-60 beams entered the chamber at angles of 15, 25, 34, 43, and 52 from the vertical axis, the chamber sensitivity for the angled entry was compared to the perpendicular entry, the geometry with which this chamber was calibrated at the ADCL. To determine the effective chamber sensitivity, a 6 MV photon beam from the Varian 600C (Palo Alto, CA) was directed to the chamber at the same angles as with RGS_u. The reading from the vertical direction was then compared to the average reading over the readings at five angles. For this measurement, the Capintec PR-05P "mini" chamber was inserted into the

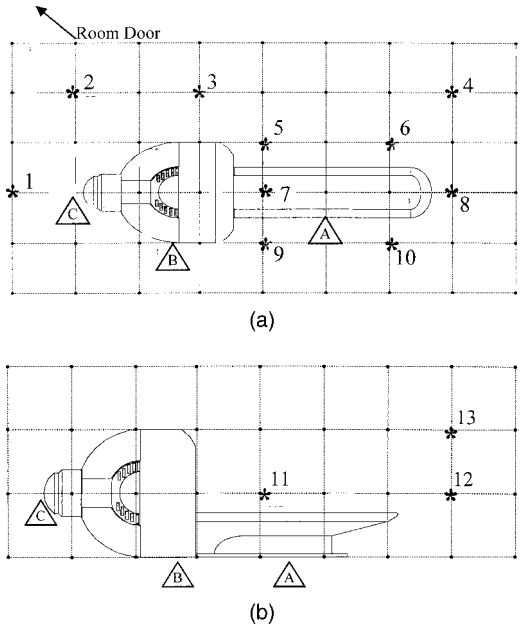

FIG. 4. Scattered radiation measurement locations: Top view (a) and side view (b). Each grid is 90 mm×90 mm. An asterisk and the corresponding number indicate where the measurement was done. The triangle points to the locations of emergency hand wheels: (A) to move the couch out to, (B) to close the shielding door and (C) to close the secondary shutter.

16-cm-diam spherical phantom. The 18 mm RGS collimator was simulated by a 17.5-mm-diam linac-based radiosurgery circular collimator insert, which was used for stereotactic radiosurgery treatment.[4] Similarly, the 14 mm RGS collimator was simulated by a 15-mm-diam circular collimator insert. The chamber measurements were not made for 8- and 4-mm-diam collimators because the nonuniform beam intensity over the chamber's sensitive volume may not be accounted for.

The absolute chamber measurements were done twice on different days and the dose in water was calculated using the TG-21 formalism,[5]

$$D_{\text{water}} = D_{\text{acrylic}} \times (\text{L}/\rho)^{\text{water}}_{\text{acrylic}} \times \text{ESC},$$

where the dose to water, D_{water}, was converted from the measured dose in acrylic, D_{acrylic}. $(\text{L}/\rho)^{\text{water}}_{\text{acrylic}}$ is the restricted stopping power ratio between water and acrylic for a Co-60 beam. ESC, the excessive scattering correction factor, (L/ρ) were extracted from the TG-21. The dose in acrylic, D_{acrylic}, was determined using the TG-21 formalism;

$$D_{\text{acrylic}} = C_{\text{tp}} * C_{\text{elec}} * C_{\text{beam}} * M * N_{\text{gas}} * P_{\text{ion}} * P_{\text{wall}} * P_{\text{repl}},$$

where C_{tp} = the temperature–pressure correction factor, C_{elec} = the electrometer correction factor, C_{beam} = the beam entry angle correction factor as discussed earlier, M = the meter reading corrected for timer error, N_{gas} = the chamber calibration factor. P_{ion}, P_{wall}, and P_{repl} are, respectively, the ion recombination correction factor, the chamber wall correction factor, and the replacement correction factor.

TLD dosimetry was based on the determination of the sensitivity of the individual TLD chips. Ten 1 mm×3 mm ×3 mm TLD chips were calibrated by exposing them to a 6

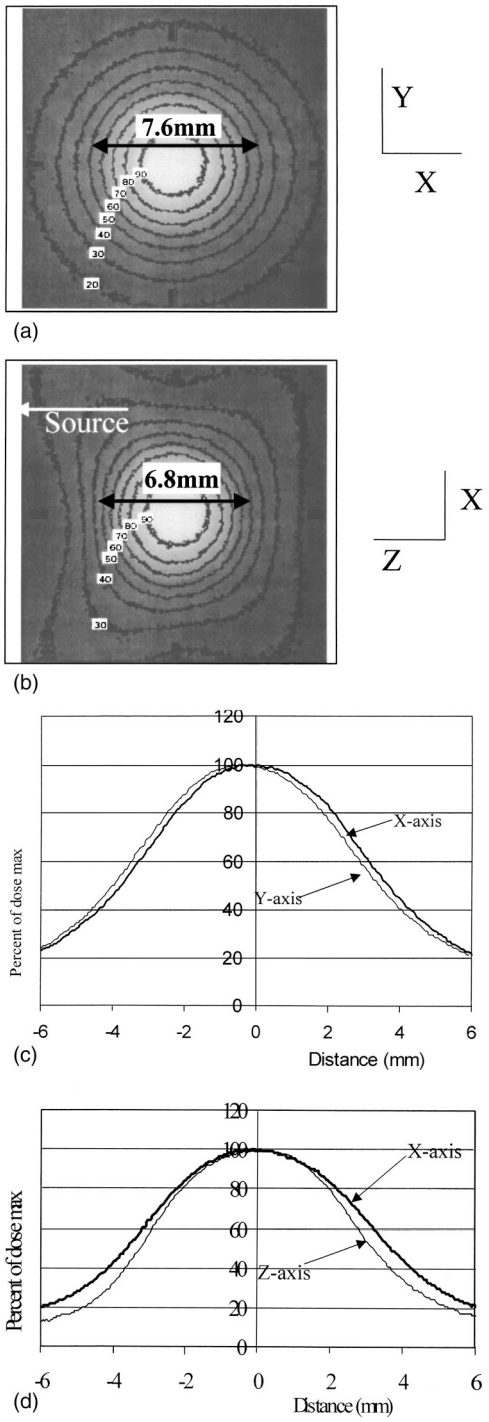

FIG. 5. Dose contours with the 4 mm collimator film exposure on the *XY* (a) and the *XZ* (b) planes. (c) The 4 mm collimator profiles on the *X* and *Y* axes of the *XY* plane and (d) on the *X* and *Z* axes of the *XZ* plane. The *Y*-axis profile in (c) is shifted to the left so that it can easily be distinguished from the *x*-axis profile. The distance indicated in (a) and (b) is the full width at 50% isodose profile in the specific direction. For example, 7.6 mm in (a) is in the *X* direction. Isodose lines of 90%, 80%, 70%, 60%, 50%, 40%, 30%, and 20% are also shown.

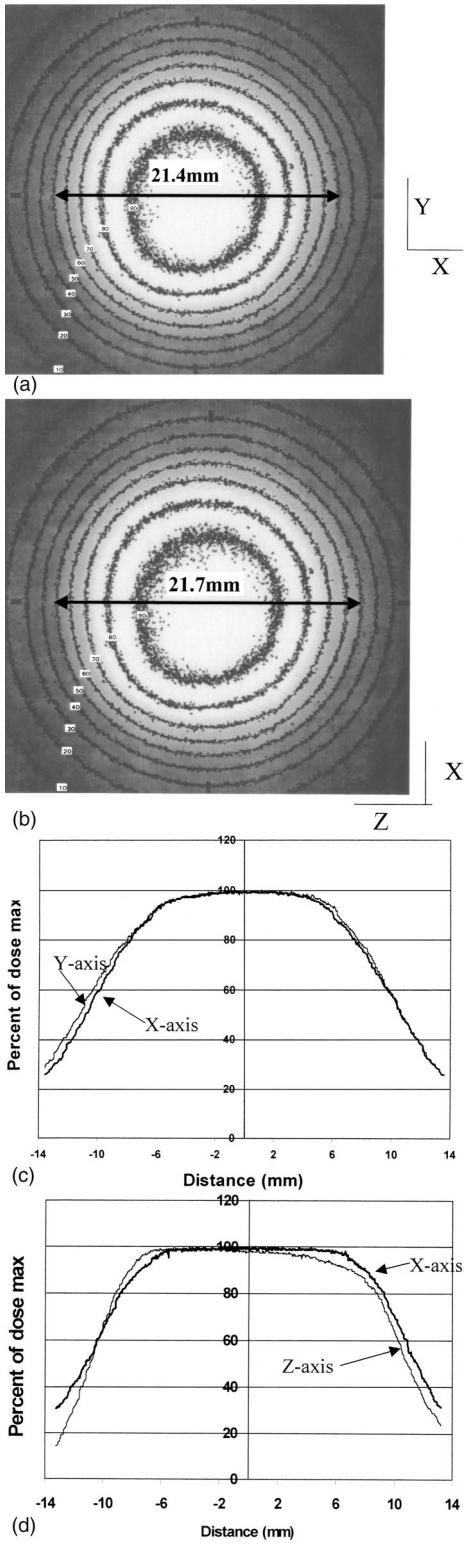

FIG. 6. Dose contours with the 18 mm collimator film exposure on the *XY* (a) and the *XZ* (b) planes. (c) The 18 mm collimator profiles in the *X* and *Y* axes of the *XY* plane and (d) in the *X* and *Z* axes of the *XZ* plane.

MV photon beam from the Varian Clinac 600C linear accelerator at the depth of dose maximum, 1.5 cm. Then, two to four of them were stacked in the *Z* direction on the beam axis inside the Capintec chamber slot in the 16-cm-diam acrylic phantom and irradiated with the RGS Co-60 beam for 15 Gy. The dose rate for the 4 and 8 mm collimators were corrected for the nonuniform dose distribution over the TLD chips. This was accomplished by averaging the peak region of the

TABLE I. The first column indicates the collimator size and the plane of the film. The data are the averages of distances in the *X* and *Y* directions on the *XY* plane and in the *X* and *Z* directions on the *XZ* plane. The units of the data are all in millimeters. The large second and third columns are the results of Goetsch's Auhai RGS_c data and our Auhai RGS_c data, respectively. The last large column shows the results of our RGS_u data. Each large column is divided into three (or four) columns, one for the full width at the 90% isodose line, one at the 50% isodose line, and one for the penumbra. The penumbra defined by Goetsch is different from the conventional definition. However, for the sake of comparison, his definition is used in this paper.

Collimator plane	Auhai RGS_c[a]			Auhai RGS_c[b]				UC Davis RGS_u[b]				
	90%	50%	Penumbra	90%	50%	Penumbra	diff	90%	50%	penumbra	diff	DIFF
4 *XY*	3.0	6.7	3.7	3.0	6.4	3.4	−0.3	3.1	7.4	4.3	0.6	1.9
4 *XZ*	2.7	6.3	3.6	2.9	6.1	3.2	−0.4	3.1	6.9	3.8	0.2	0.4
8 *XY*	6.3	12.0	5.7	7.1	11.9	4.8	−0.9	4.0	10.0	6.0	0.3	2.9
8 *XZ*	6.2	11.4	5.2	7.2	11.4	4.2	−1.0	5.2	10.0	4.8	−0.4	0.3
14 *XY*	11.7	18.5	6.8	12.6	19.1	6.5	−0.3	10.1	18.3	8.2	1.4	3.8
14 *XZ*	11.1	17.4	6.3	12.5	18.1	5.6	−0.7	12.2	17.9	5.8	−0.5	−0.5
18 *XY*	15.7	23.1	7.4	16.0	23.4	7.4	0	12.7	21.8	9.1	1.7	1.7
18 *XZ*	14.9	22.1	7.2	15.6	22.1	6.5	−0.7	15.6	22.3	6.7	−0.5	−0.5

[a]Reference 1.
[b]Present work.

dose profiles over 3 mm in the *X* and *Y* directions. Subsequently the remaining control group chips were irradiated for 15 Gy using the 6 MV photon beam in the same manner as the relative sensitivity measurements. These ten TLD chips were read at one setting with a Victoreen TLD reader model 2800M (Cleveland, OH). By comparing the relative sensitivity of all TLD chips, the relative response difference between 6 MV photons and Co-60 gamma rays,[6] and the actual TLD response to the RGS beams, the dose rate of the RGS system at the focal point within the 16-cm-diam acrylic phantom was determined. For 4 and 8 mm collimators, two chips were stacked whereas for the 14 and 18 mm collimators, four chips were used. The timer error of −0.05 min, which was separately determined, was accounted for in the dose-rate determination.

The third indirect dosimetry comparison was made by irradiating the TLD powder in the MD Anderson stereotactic head phantom using the 18 mm collimator. The phantom was first CT scanned with a light radio-opaque marker as the target. The marker container was replaced with the same size TLD powder container in the same location as the radio-opaque marker. The TLD irradiation time was based on the dose rate determined for the 18 mm collimator by the chamber method described previously. This TLD result did not necessarily determine the machine output, but reflected the combined accuracy of the treatment planning unit and the machine output.

B. Collimator output factors

In addition to the chamber and TLD measurements for the collimator output factors, a Gafchromic film MD-55 was also irradiated with each of the four collimator sizes. A Gafchromic film sandwiched by two 5-mm-thick flat plastic plates, which were snuggly fit into a slot made in the 16-cm-diam acrylic phantom, was exposed. Two films were exposed for each of the four collimator sizes; one on the *XY* plane and the other on the *XZ* plane. (*X, Y*, and *Z* directions correspond to lateral, anterior-posterior, and superior-inferior directions in the patient coordinates.) The film exposure time was calculated using the published output factors[1] so that the film density in the central axis was approximately equal in all films. For the 18 mm collimator, the film was exposed for 1000 s. The collimator output factor was proportional to the ratio of the average film density on the central axis to the exposure time. This ratio was normalized to that for an 18 mm collimator size. The average density on the central axis was the average film density over a small region of the *X, Y*, and *Z* axes. This region ranged from 0.3 mm^2 for the 4 mm collimator, 0.5 mm^2 for 8 mm, to 0.9 mm^2 for 14 and 18 mm collimators. The film density was determined at the UW-ADCL. The same set of films were also scanned in-house using Lumiscan 150 by Lumisys (Tucson, AZ) and the accuracy of Lumisys was measured against the UW-ADCL scanner. Subsequent film scans were done in-house.

The collimator output factors were also measured with the A14SL chamber by replacing the Capintec chamber in the 16-cm-diam acrylic phantom. The chamber has an active volume of 0.009 cc. The chamber's active volume is defined by a near half dome, and is 2 mm along the chamber axis and 4 mm diameter. When the chamber was irradiated by beams ranging from 15° to 52° from the chamber's vertical axis, the

TABLE II. Collimator output factors. The first column gives the size of the collimator. The published results are given in the second column. The next four columns give the results obtained with the Capintec chamber, Shonka A14SL chamber, TLD, and Gafchromic films using RGS_u. The normalized outputs from RGS_u and RGS_c are consistent among the four methods for 18 and 14 mm collimators.

Collimator (mm)	Auhai RGS_c	UC Davis RGS_u			
	Goetsch *et al.*[a]	Capintec chamber	A14SL chamber	TLD	Gafchromic film
18	1.000	1.000	1.000	1.000	1.000
14	0.982	0.975	0.975	0.984	0.980
8	0.937		0.861	0.912	0.844
4	0.610		0.604[b]	0.593	0.583

[a]Reference 1.
[b]No chamber volume insufficient coverage was corrected (see the text).

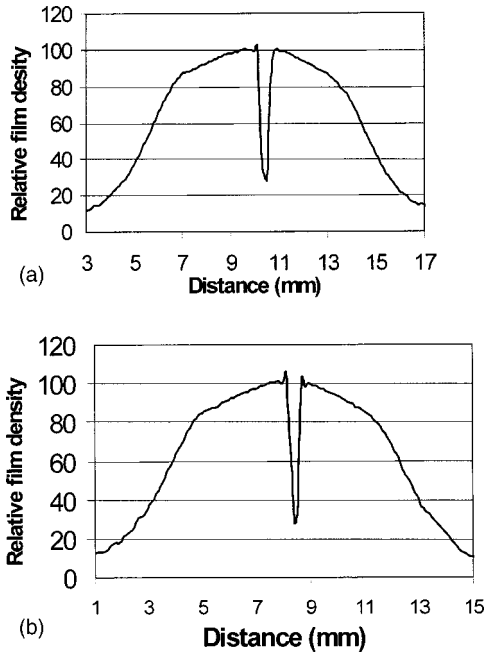

FIG. 7. Mechanical accuracy of the RGS_u. Pinprick results obtained with the 4 mm collimator. (a) and (b) correspond to the scans in the *X* and *Y* directions of the *XY* plane, respectively.

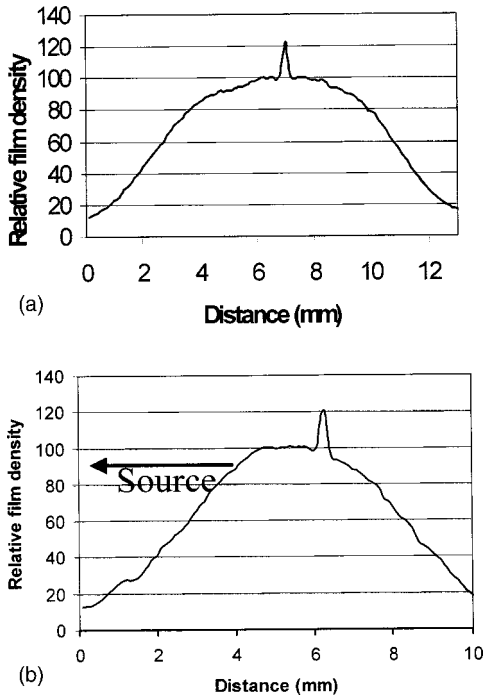

FIG. 8. Pinprick results obtained with the 4 mm collimator. (a) and (b) correspond to the scans in the *X* and *Z* directions of the *XZ* plane, respectively.

active volume will be covered by a 2.5-mm-diam beam for the 15° entry and 3.5 mm for the 52° beam entry. The chamber diameter perpendicular to the beam direction is still 4 mm. Therefore, the chamber will be completely covered by the beams from 8, 14, and 18 mm collimator. The 4 mm collimated beam may not completely cover the active volume. Since we do not know how to correct the chamber volume insufficient coverage, no such correction was made for the 4 mm collimator.

C. Mechanical and radiation center accuracy

An approach to determine the mechanical accuracy of RGS is to measure the coincidence between the mechanical focal spot and the radiation center using a vendor supplied pinprick device. The pinprick device is made of aluminum, coated with a scratch resistant material. The device has a 2.5 cm×3.0 cm×0.1 cm deep indentation on a 5-cm-diam semicylinder. A 4 cm×5 cm×0.2 cm thick aluminum cover plate with a matching 2.5 cm×3.0 cm×0.1 cm protrusion fits in the indentation. Together they hold the film firmly. The device comes with a pin, which will prick the film. The prick mark on the film is the mechanical center of the RGS unit. The film was exposed to 15 Gy using the 4 mm collimator. The distance between the pinprick mark and the center of the irradiated field defined at the half maximum was determined by the Lumiscan 150. The pinprick device was rotated so that the film was exposed either in the horizontal plane (*XZ* plane) or in the vertical plane (*XY* plane).

D. Timer errors, timer accuracy, and timer linearity

Using the absolute dose measurement setup, the Capintec PR-05P chamber was exposed to the timer set at 1, 4, and 10 min. To reduce the statistical uncertainty, the 1 and 4 min readings were repeated four times. Their averages and one 10 min reading were fit with a linear equation;

$$R = A*(t+B),$$

where R is the reading, A is the dose rate; t is the measuring time, and B is the timer error. The timer error, B, is also calculated using the average readings from 1 and 4 min exposures, R_1 and R_4, as

$$B = (4*R_1 - R_4)/(R_4 - R_1),$$

The timer accuracy was measured against a stopwatch; During the 10 min exposure, the stopwatch started when the treatment console's digital clock indicated time at *A*. When the digital clock indicated $A+5$ min, the watch was stopped. The stopwatch indicated 5 min$\pm$1 s out of three tries.

E. Leakage and scattered radiation

Leakage radiation at and around the RGS source shield and the scattered radiation in the room were measured using a Bicron/Eberline model C801B ion chamber. The leakage radiation was measured at approximately 1 m from the location of the source cluster with the source shield door closed and the source being in the "home position." The scattered radiation was measured with the Rando head and body phantom on the couch in the treatment position. To maximize the scattered radiation, the largest collimator of 18 mm was used. For scattered radiation, only the representative spots on the horizontal plane at the height of the focal spot and on the vertical plane defined by the source rotation axis were measured. Figure 3 shows the top [Fig. 3(a)] and side [Fig. 3(b)]

TABLE III. Mechanical accuracy of the RGS units. No data in the *Z* direction were obtained by Kubo at Auhai. "Diff1" shows the difference between Goetsch and Kubo for RGS_c. "Diff2" is the difference between RGS_c by Goetsch and RGS_u. The numbers in parentheses indicate the collimator size.

Auhai RGS_c[a]	Auhai RGS_c[b]	Diff1	UC Davis RGS_u[b]	Diff2
0.23 mm (4 and 8 mm)	*X* and *Y*: 0.31 mm (4 mm only)	+0.08 mm	*X* and *Y*: 0.29 mm (4 mm only) *Z*: 0.75 mm (4 mm only)	+0.06 mm

[a]Reference 1.
[b]Present work.

views of the source shielding body and the measurement points on the circumference at approximately 1 m from the source cluster. The numbers along the circumference are the measurement-point location numbers. Location 3 and 7 are symmetric about the source rotation axis as are locations 2 and 8, and 4 and 6. For the side view, location 1 is in the back of the RGS unit on the source rotation axis. Point *a* is located 45° clockwise from location 1. Location *b* is another 45° clockwise rotation from location *a*. Location *b* is for information only since the leakage at location *b* cannot be measured. The two location numbers in the center of the diagram indicate the opposing locations.

Figures 4(a) and 4(b) show the top and side views of the room where the scattered radiation was measured. The room entry door is located on the upper left-hand side corner in Fig. 4(a). The measurement was mainly obtained near or on the couch simply because the reading beyond these points was found to decrease rapidly as the measurement point moves further away.

III. RESULTS

A. TLD, film, chamber, MD Anderson phantom

Absolute dosimetry. The ionization chamber measurements resulted in the dose-rate output of 3.00 Gy/min in the center of the 16-cm-diam acrylic phantom. The TLD measurement gave rise to the average dose rate of 2.94 Gy/min over two measurements. The MD Anderson stereotactic phantom data yielded 3.13 Gy/min. The beam entry angle correction factors of the Capintec PR-05P chamber for the 18 and 14 mm collimators were measured to be 0.993 and 0.990, respectively. A similar factor for the A14SL chamber for the 8 mm collimator was 0.99. The correction factors for the TLD response between a Co-60 and 6 MV x-ray beam were reported to be 0.989 by measurement and 0.991 by Monte Carlo calculation.[6] Therefore the average value of 0.99 was used in this work.

B. Dose profiles and collimator output factors

1. Dose profiles

The results of profile comparison between the Lumiscan and UW-ADCL scanner are summarized as the following. Though the results are not shown, the difference was derived from the full 50% width between the two scanner results. For 4, 8, 14, and 18 mm collimators, the average difference over combined *X* and *Y* directions in the *XY* plane was within 0.1, 0.0, 0.0, and 0.3 mm, respectively. Similarly, the differences over the combined *X* and *Z* directions in the *XZ* plane were within 0.1, 0.1, 0.2, and 0.2 mm. The penumbra defined as the difference in full width between the 90% and 50% isodose lines for 4, 8, 14, and 18 collimators were within 0.1, 0.3, 0.3, and 0.2 mm in the *XY* plane and 0.1, 0.0, 0.3, and 0.0 mm in the *XZ* plane. The same 18 mm collimator films were scanned by Lumiscan 150 at two-month intervals. The 50% widths for the 14 and 18 mm collimator averaged over the combined *X* and *Y* axes in the *XY* and over the combined *X* and *Z* axes in the *XZ* plane were within 0.3 and 0.2 mm, respectively. The penumbra differences were 0.1 and 0.1 mm in the *XY* and *XZ* planes. Therefore, It can be concluded that the Lumiscan can be used in place of the UW-ADCL scanner.

The film isodose plots supplied by the UW-ADCL are shown in Figs. 5(a) and 5(b), and 6(a) and 6(b), respectively, showing the results of 4- and 18-mm-diam collimator dose contours in the *XY* and *XZ* planes. The small numbers overlaid on the graphs show the percent isodose plots. The large numbers indicate the distance for the full width at a 50% dose level. Figure 5(a) shows circular isodose curves whereas Fig. 5(b) shows isodose curves extending from the center of the graph toward the four corners, or horns. These horns are created by the beam entering and leaving the horizontal film at angles between 15° and 52° from the vertical axis. In this graph, the left-hand side is superior where the sources are located, thus getting more radiation than the right-hand side. The horns for the 18-mm-diam collimator are washed out by the larger size beams and are not delineated [Fig. 6(b)]. There is no horn on the film placed vertically since the beam contribution to the film is symmetric about left–right or anterior–posterior. The beam profile scans are shown in Figs. 5(c) and 5(d), and 6(c) and 6(d). For *X* and *Y* axis scans of the *XY* plane, the profiles in both directions are almost identical for both collimator sizes. The profile on the *Z* axis is narrower than those on the *X* and *Y* axis profiles.

Table I shows the various average distances of profiles in the *X* axis and *Y* axis in the *XY* plane (or *X* axis and *Z* axis in the *XZ* plane.) It summarizes the full width at 90% and 50% isodose lines, and the penumbra (the difference in the full widths between the two isodose lines) from all eight planes.

TABLE IV. Results of leakage radiation measurement in units of mR/h.

Location No.	1	2	3	4	5	6	7	8
Fig. 3(a), top view (horizontal plane)	0.06	0.16	0.12	0.35	6.0	0.15	0.15	0.12
Location No.	1	a	b	c	5	d	e	f
Fig. 3(b), side view (vertical plane)	0.06	3.5	NA	0.34	6.0	0.35	0.06	0.2

This parametrization of the penumbra may not be accurate due to the presence of sloping shoulders at 90% as seen in the *Z*-axis profile of the 18 mm collimator [see Fig. 6(d)]. The column labeled "diff" shows the difference in the penumbra between the results of Goetsch *et al*. and our RGS_c or RGS_u results. The present RGS_c results show slightly smaller penumbra (negative value). In general, the RGS_u penumbra in the *XY* (or *XZ*) plane is larger (or smaller) than the RGS_c penumbra. The last column "DIFF" indicates the difference between our RGS_u and the Gamma-Knife penumbra data.[1] The RGS_u shows slightly larger penumbra than the Gamma-Knife in the *XY* plane. The penumbra is approximately equal in the *XZ* plane.

2. Collimator output factors

Table II summarizes the results of collimator output factors. All data are normalized to the 18 mm collimator output. The results are consistent between the two methods for the 4 mm collimator. For the 8 mm collimator, UCD's Gafchromic results are similar to the results with the A14SL chamber and approximately 9% lower than the remaining two other results. During the course of the TLD study, the TLD reader's power supply was found to be malfunctioning and irreparable. Therefore, we have no way of retesting the TLD dosimetry.

C. Mechanical accuracy

Figures 7(a) and 7(b) show the results of the pinprick film scan obtained from RGS_u in the *X* and *Y* directions of the *XY* plane. The distance between the pinprick marker and the center of the radiation field defined at 50% is approximately 0.3 mm. Figures 8(a) and 8(b) show similar scans in the *X* and *Z* directions of the *XZ* plane. The distance difference in the *X* direction in this example is approximately 0.3 mm. However, the center of the radiation field in the *Z* direction is shifted toward the source [left-hand side of Fig. 8(b)] by 0.75 mm. The distance accuracy of the scanner was better than 0.1 mm by scanning two markers separated by 5 cm. Table III lists the published as well as our results on the mechanical accuracy of the RGS units. Our RGS_c and RGS_u results are based only on the 4 mm collimator. "Diff1" is the difference between Goetsch and the present work on the Auhai unit. "Diff2" is the difference between Goetsch's results and our RGS_u results. For the collimator sizes of 4 and 8 mm, all results show the mechanical accuracy of approximately 0.3 mm or less. The variations between different investigators or between the two different RGS units were found to be small.

TABLE V. Results of scattered radiation measurements.

Location in Fig. 4(a)	Reading (R/h)	Location in Fig. 4(b)	Reading (R/h)
1	0.0006	11	11.9
2	0.002	12	2.0
3	0.006	13	1.0
4	0.75		
5	0.25		
6	0.1		
7	11.6		
8	2.0		
9	0.1		
10	2.0		

The exception is the accuracy of RGS_u in the *Z* direction, which is more than twice those in the other two directions. Unfortunately, there is no other report on the results for the *Z* direction.

D. Leakage and scattered radiation

Since the source geometry was not axially symmetric, the reading in a given location varied as the source rotated. Therefore, the scattered radiation was an average of the largest and smallest readings.

1. Leakage radiation

As seen from Table IV, the highest leakage radiation of 6.0 mR/h was observed at the couch side of the source rotation axis. The next highest reading of 3.5 mR/h was observed at location *a*, which is close to the source home position. All the other readings were less than 0.6 mR/h. Though not listed in Table IV, the readings next to the shielding door were approximately 20 mR/h.

2. Scattered radiation

The highest reading was approximately 11.6 R/h at location 7 in Fig. 4(a) and 11.9 R/h at 11 in Fig. 4(b). The reading fell rapidly away from the rotation axis. Location 4 was 0.75 R/h whereas locations 2 and 3 were 0.002 and 0.006 R/h, respectively (Table V).

IV. DISCUSSION

It is found that the absolute dose difference among all dosimetry systems for the 18 mm collimator is within 6%. There are several articles dealing with small field dosimetry, in particular for the Gamma-Knife.[7–10] As for the Gamma-Knife collimator output factors, there is clear evidence that the results reported in Refs. 7–9 are in good agreement for all collimator sizes. From Table IV of Ref. 9, the collimator output factors of the Gamma-Knife range from 0.82 to 0.9, 0.94 to 0.95, 0.97 to 0.99, and 1.000, respectively, for 4, 8, 14, and 18 mm collimators. The RGS results for 4 and 8 mm are quite different from these data and are approximately 0.6 and 0.85, smaller than the corresponding Gamma-Knife results. Whether these differences have anything to do with the size of the source, or the source configuration is not known.

Monte Carlo calculations may be one approach to shed light on the determination of the collimator output factors of RGS. We intend to investigate the smaller collimator output factor measurements with a small volume chamber and a MOSFET detector in the future.

The nonflat profile in the *Z* direction in the *XZ* plane is evident in Figs. 6(d) and 8(b). The higher density on one side of the shoulder is a manifestation of that side being closer to the sources, which are located to the left of the figures in all cases. This also explains the fact that the discrepancy of the mechanical and radiation coincidence is larger in the *Z* direction and the radiation center is shifted toward the source by 0.75 mm [Fig. 8(b)].

V. CONCLUSION

The dosimetry and mechanical accuracy of the modified RGS are found to be similar to those of the original RGS. Since it is reported[1] that these quantities are similar between the original RGS and Gamma-Knife, it may be said that the modified RGS should behave similarly in terms of dosimetric and mechanical accuracy to the Gamma-Knife.

ACKNOWLEDGMENTS

The authors acknowledge the assistance received from Kal Nawawi and Franz Krispel of OUR Scientific, Inc., during the measurements.

[a]Author to whom all correspondence should be addressed; electronic mail: hdkubo@ucdavis.edu

[b]On leave from College of Medical Sciences, Kumamoto University, Kumamoto, Japan.

[1] S. J. Goetsch *et al.*, "Physics of rotating gamma systems for stereotactic radiosurgery," Int. J. Radiat. Oncol., Biol., Phys. **43**, 689–696 (1999).

[2] W. McLaughlin *et al.*, "The use of a radiochromic detector for the determination of stereotactic radiosurgery characteristics," Med. Phys. **21**, 379–388 (1994).

[3] A. Niroomand-Rad *et al.*, "Radiochromic film dosimetry: Recommendations of AAPM Therapy Committee Task Group 55," Med. Phys. **25**, 2093–2115 (1998).

[4] H. D. Kubo, C. T. E. Pappas, and R. B. Wilder, "A comparison of arc-based and static mini-multileaf collimator-based radiosurgery treatment plans," Radiother. Oncol. **45**, 89–93 (1997).

[5] Task Group 21, Radiation Therapy Committee, American Association of Physicists in Medicine, "A protocol for the determination of absorbed dose from high-energy photon and electron beams," Med. Phys. **10**, 741–771 (1983).

[6] P. N. Mobit, P. Mayles, and A. E. Nahum, "Quality dependence of LiF-TLD in megavoltage photon beams: Monte Carlo simulation and experiments," Phys. Med. Biol. **41**, 387–398 (1996).

[7] P. S. Nizin and R. B. Mooji, "Tissue-air ratios for ^{60}Co gamma-ray beams," Med. Phys. **25**, 1458–1463 (1998).

[8] A. Wu *et al.*, "Physics of Gamma-Knife approach on convergent beams in stereotactic radiosurgery," Int. J. Radiat. Oncol., Biol., Phys. **18**, 941–949 (1990).

[9] P. S. Nizin, "On absorbed dose in narrow ^{60}Co gamma-ray beams and dosimetry of the Gamma-Knife," Med. Phys. **25**, 2347–2351 (1998).

[10] L. Ma, X. A. Li, and C. X. Yu, "An efficient method of measuring the 4 mm helmet factor for the Gamma-Knife," Phys. Med. Biol. **45**, 729–733 (2000).